# Lipschitz Regularized CycleGAN for Improving Semantic Robustness in Unpaired Image-to-image Translation

Zhiwei Jia\* UC San Diego Bodi Yuan\* X

Kangkang Wang X Hong Wu X

zjia@eng.ucsd.edu

bodiyuan@google.com

kangkang@google.com

wuh@google.com

David Clifford X Zhiqiang Yuan X

Hao Su UC San Diego

davidclifford@google.com

zyuan@google.com

haosu@eng.ucsd.edu

# **Abstract**

For unpaired image-to-image translation tasks, GAN-based approaches are susceptible to semantic flipping, i.e., contents are not preserved consistently. We argue that this is due to (1) the difference in semantic statistics between source and target domains and (2) the learned generators being non-robust. In this paper, we proposed a novel approach, Lipschitz regularized CycleGAN, for improving semantic robustness and thus alleviating the semantic flipping issue. During training, we add a gradient penalty loss to the generators, which encourages semantically consistent transformations. We evaluate our approach on multiple common datasets and compare with several existing GAN-based methods. Both quantitative and visual results suggest the effectiveness and advantage of our approach in producing robust transformations with fewer semantic flipping.

# 1. Introduction

Unpaired image-to-image translation is a very challenging task. In an unsupervised manner, one aims to learn a joint distribution of images from two or more domains by only accessing images from marginal distributions of their individual domains. This problem setup intrinsically introduces ambiguities since multiple statistically very different joint distributions can exist that produce the same marginal one. Consequently, additional assumptions about the transformation are necessary. Various types of inductive bias have been introduced to produce convincing mappings from the human perspective.

As one of the most widely used assumptions on this subject, cycle consistency [71] suggests that the ideal mappings between the two domains are bijective and therefore

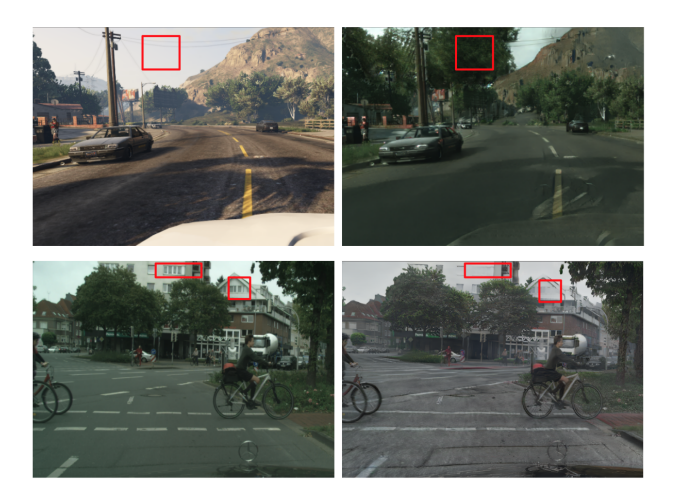


Figure 1. Failure cases of transforming GTA images to Cityscapes via CycleGAN. Top row: a GTA image (left) is translated into the Cityscapes style (right). Bottom row: translation in the opposite direction. Boxes in red highlight the semantic flipping, which is partially due to the different semantic statistics between GTA and Cityscapes (more trees & buildings in Citysacpes).

information-preserving. This assumption is not sufficient since a permutation of the mappings would not violate the constraint. Also, as pointed out in [13], CycleGAN can learn to hide information such that a technically bijective mapping still loses key information from the human perception perspective. To deal with this, semantic consistency such as the ones in [24, 59] are introduced to enforce similarity between input and output images. These approaches require either extra training inputs or pre-trained models that are not available for general image translation tasks. A promising alternative is to learn these metric functions unsupervisedly in a contrastive fashion, as in [38, 45]. However, without knowing the ground truth correspondence, any similarity enforcement between input and output images

<sup>\*</sup>Co-first authors; most work done during Zhiwei Jia's internship at X.

might be misleading. An intuitive approach that avoids this is to ensure intra-domain similarity preserving [8, 68] so that visual distances between source images are reflected among their corresponding target images. Nevertheless, the existing methods can be too restrictive that leads to serious artifacts (see Sec. 3.5 for a detailed discussion).

In this paper, we specifically tackle one type and also a major type of errors made in translations - the semantic flipping as illustrated in Fig. 1. We provide and analyze two underlying reasons for this phenomenon in Sec. 3.2. Namely, (1) the mismatching semantic statistics between source images and target images, which is prevalent for unpaired image translation tasks, and (2) the over-expressiveness of the generators that leads to their inconsistent translations and susceptibility to noises. We then introduce our proposed solution in Sec. 3.3 as L-CycleGAN, namely, CycleGAN with Lipschitz regularized generators. In Sec. 3.4 & 4, we show that, although a simple approach, L-CycleGAN can improve semantic robustness and effectively reduce semantic flipping. Our method outperforms several baselines both qualitatively and quantitatively on 5 common datasets.

#### 2. Related Work

Generative Adversarial Networks (GANs) Since the introduction of the original GAN by [20], a wide range of its applications have been proposed in areas such as image manipulations, image synthesis, audio synthesis, style transfer, domain adaptation, adversarial defence and data augmentation [16, 66, 50, 24, 31, 10, 36, 46, 53, 2]. The central idea of adversarial learning is to minimize the statistical difference, measured using the discriminators, across domains via updating the generators. Many improvements were made for the architecture structures [49, 32, 66, 33, 65, 28], the statistical distance and the induced loss function used during training [3, 12, 44, 42, 48, 70]. Some of the existing work such as Wasserstein GAN [3] also propose Lipschitz constraints. While they are all applied on the discriminators, our proposed regularizer focuses on the generators for a completely different purpose.

**Image-to-image Translation** In paired image-to-image translation, models are learned with direct pixel-level supervision. Work such as [17, 51, 28, 63] achieves good results on various datasets that contain well-aligned input and ground truth images. Recent advances have been made in unpaired image-to-image translation, which is more challenging but also more practical. In specific, cycle consistency has been vastly used to generate more convincing translations [37, 71, 34]. On the other hand, [27, 39, 40] perform translation by learning shared cross-domain latent representation of the images.

Preserving Semantics in Image Translation In unpaired image translation, it is critical to preserve the semantic content of the source images since no correspondence information is provided during training. There are several existing approaches. Cycle consistency [71] is proposed to enforce bijective mappings between domains so that semantic information will not be lost during translation. Geometry consistency [19] enforces equivariance of the generators regarding geometric transformations. DistanceGAN [8] and HormonicGAN [68] encourages visual similarities within the source domain to be reflected in the target domain (see Sec. 3.5 for a comparison between these methods and ours). Multiple work [59, 9, 54, 38, 45] adopt the idea that input and output images should be similar, measured by a function either pre-defined or learned contrastively.

Robustness & Generalization of DNNs Semantic robustness and semantic flipping discussed in our paper are related to both adversarial robustness and generalization ability. Some work has tackled the adversarial robustness of GANs [13, 7, 61]. And some [67, 60, 4] has explored their generalization properties. In a broader context, both adversarial attack and defense have been extensively studied [56, 22, 26, 58, 57, 47, 21, 1], and many recent advances have been made for understanding the generalizability of DNNs [43, 55, 64, 6, 69, 18, 5, 30, 29].

#### 3. Method

#### 3.1. Preliminaries

The goal of unpaired image-to-image translation is to learn functions between two domains X and Y given training samples  $\{x_i\}_{i=1}^N, \{y_j\}_{j=1}^M$  where  $x_i \in X, y_j \in Y$ . We denote the data distribution as  $x \sim p_X(x)$  and  $y \sim p_Y(y)$ . To learn the two mappings across the domain, namely  $G: X \to Y$  and  $F: Y \to X$ , two adversarial discriminators  $D_X$  and  $D_Y$  are applied, where  $D_X$  aims to distinguish between images  $\{x\}$  and translated images  $\{F(y)\}$  and  $D_Y$  to distinguish between  $\{y\}$  and  $\{G(x)\}$ . Normally the training objective consists of multiple pieces. The first part is the adversarial losses [20], Eqn. 1 & 2, for matching the marginal distribution of generated images to that of the target domain in both directions.

$$\mathcal{L}_{GAN}(G, D_Y, X, Y) = \mathbb{E}_{y \sim p_Y(y)} \left[ \log D_Y(y) \right] + \mathbb{E}_{x \sim p_X(x)} \left[ \log \left( 1 - D_Y(G(x)) \right] \right]$$
(1)

$$\mathcal{L}_{GAN}(F, D_X, X, Y) = \mathbb{E}_{x \sim p_X(x)} \left[ \log D_X(x) \right] + \mathbb{E}_{y \sim p_Y(y)} \left[ \log \left( 1 - D_X(G(y)) \right) \right]$$
(2)

Clearly, the translation requires to perverse desired contents, not just converting an image to a random image from







Figure 2. An example of how cycle consistency is well enforced in CycleGAN training without effectively preventing content flipping. Left: an input GTA image; middle: the transformed image in Cityscapes style; right: the image transformed back to GTA style.

the other domain. CycleGAN performs this in a clever way by adding the cycle consistency loss [71], shown below, as the second part of the training objective.

$$\mathcal{L}_{\text{cyc}}(G, F) = \mathbb{E}_{x \sim p_X(x)} [\|F(G(x)) - x\|_1] + \mathbb{E}_{y \sim p_Y(y)} [\|G(F(y)) - y\|_1]$$
(3)

In specific, cycle consistency enforces that the learned mappings G and F are inverse functions to each other, which prevents the translation process from losing semantic information. Notice that for better image quality and training stability, CycleGAN [71] adopts LSGAN [42] whose adversarial loss is of the form  $\mathbb{E}_{y \sim p_Y(y)} \left[ (D(y) - 1)^2 \right] + \mathbb{E}_{x \sim p_X(x)} \left[ D(G(x))^2 \right]$  and also an (optional) identity loss

$$\mathcal{L}_{\text{identity}}(G, F) = \mathbb{E}_{y \sim p_Y(y)} [\|G(y) - y\|_1] + \mathbb{E}_{x \sim p_X(x)} [\|F(x) - x\|_1]$$
(4)

# **3.2.** An Existing Challenge and Its Analysis for GAN-based Unpaired Image Translation

In this paper, we try to tackle a major challenge of unpaired image translation that we called "semantic flipping". Namely, GAN-based approaches such as CycleGAN [71] tend to add extra / remove objects, patterns or in general semantic information from the original image during the transformation process. For instance, as in Figure 1, when transforming GTA images [52] to Cityscapes ones [14], CycleGAN adds trees (or leaves) to the sky, making the resulting image deviated semantically from the original one. This is mainly due to two reasons: the source and target domain have different semantic statistics and the excessive flexibility of the generators.

# 3.2.1 Difference in Semantic Statistics Across Domains

For unpaired image translation, one has to make assumptions about the underlying latent structure of the image distribution  $p_X(x)$  and  $p_Y(y)$ . Here we assume that with low-dimensional support, a domain-invariant semantic space denoted Z exists that connects the source and target domain. In specific, suppose the invertible ground truth translation functions from the semantic space to the two domain are  $h_1:Z\to X$  and  $h_2:Z\to Y$ , respectively. Accordingly

we can define the distribution  $p_Z(h_2^{-1}(y))$  and  $p_Z(h_1^{-1}(x))$  as the underlying semantic distributions w.r.t. the source and target domain. We refer to the statistics of  $p_Z$  as semantic statistics.

Denote the class of all generators parametrized by a neural network architecture of our choice as  $\{G_w\}$ . Our goal is to find the best generator  $G^*$  out of  $\{G_w\}$  such that  $p_Y(G^*(x))$  approximates  $p_Y(y)$  as well as possible provided that the semantic information is also preserved. Ideally  $G^*$  is the function approximating  $h_2 \circ h_1^{-1}$  the best and  $F^*$  approximating  $h_2^{-1} \circ h_1$ . However, during GANbased training, we learn them by matching  $p_Y(y)$  with  $p_Y(G_w(x))$ , whose optimal solution  $G^*$  might be far from the supposed ground truth translation functions, even with cycle consistency enforced. The learned mappings might be permutations of the ground truth functions, a problem empirically can be alleviated by the identity loss (Eqn. 4). A much more challenging issue is that, even with the ground truth functions, usually the two distribution  $p_Y(h_2 \circ h_1^{-1}(x))$ and  $p_Y(y)$  are not marginally well matched. The nature of unpaired image-to-image translation can lead to the semantics statistics of  $p_Z$  between the two domains often differing a lot. As a result, the original training objective might be very biased that gives rise to generators with a lot of semantic flips. For instance, there are way more trees & buildings in Cityscapes [14] than in GTA [52], CycleGAN consequently forces semantic flipping as in Figure 1 to perform distribution matching.

# 3.2.2 The Excessive Expressiveness of the Generators

Does cycle consistency help to alleviate the semantic flipping issue? On the contrary, it might even aggravate this problem. As pointed out in [13], although cycle consistency enforces that the generator is invertible so that no semantic information is lost during translations, CycleGAN learns to use one generator to encode information imperceptibly and decode it accurately by another generator. By this means, it "cheats" to satisfy the cycle consistency constraint while from the human perspective the important semantic information is not preserved well in translations.

We argue that this excessive expressiveness of the generators is another major attribution of the semantic flipping

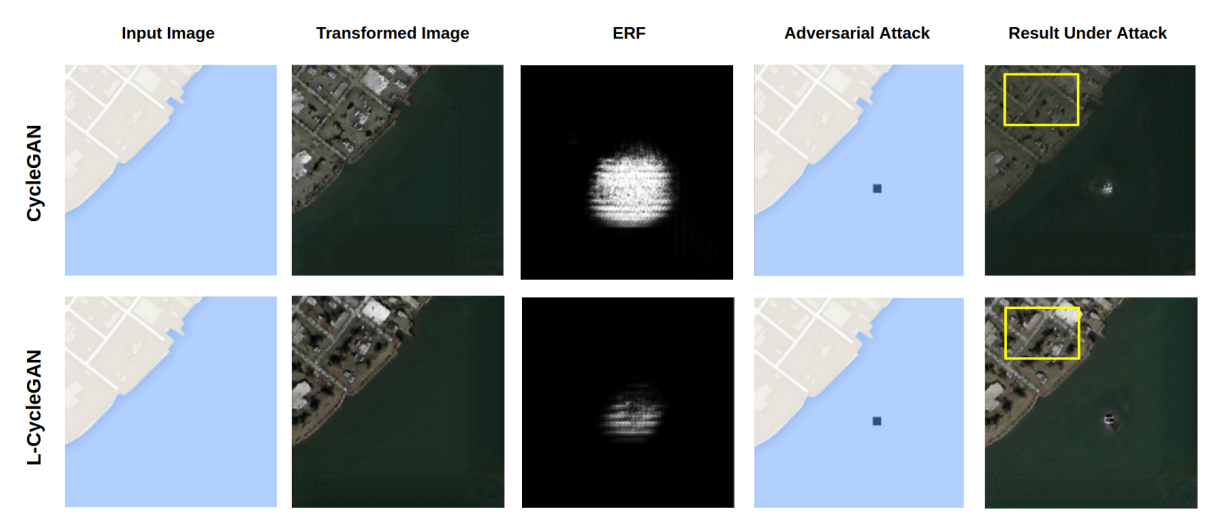


Figure 3. The effective receptive field (ERF) is reasonably smaller for L-CycleGAN, which leads to improved robustness even in the presence of an adversarial attack. The ERF of CycleGAN is, in fact, even larger than illustrated here. This not only encourages semantic flipping but also causes degraded performance in the area (e.g., highlighted in yellow boxes) far from the small adversarial object.

problem. Take Figure 2 as an example. The generators can still recover the original image from a flipped one almost perfectly. This property not only leads to the loss of desired correspondence in the translation but also makes Cycle-GAN vulnerable to noises. Furthermore, CycleGAN tends to exploit its generators' expressiveness to introduce more semantic flipping in pursuit of distribution matching. Following the previous section, when certain patterns, parts or objects are less frequent in the semantic space of the source domain than that of the target domain, a generator will manipulate the source images to forcibly merge semantically different regions into those of the same semantic meaning. If it is in the opposite scenario, a generator will split the semantically similar regions to compensate for the difference in semantic statistics between the two domains. These are well exemplified in Figure 1.

We refer to the robustness of the generators with respect to perturbations on the semantics of the source images as the semantic robustness. With improved semantic robustness, the flipping can be drastically reduced as it becomes harder for CycleGAN to hide semantic information and therefore the cycle consistency constraint becomes more effective.

#### 3.3. Lipschitz Regularization on the Generators

We can tackle the semantic flipping problem by dealing with the two issues illustrated above. The first one is very hard as it is related to the nature of unpaired image translation and we might have no knowledge of the semantic statistics of the two domains. The second one is easier to handle and there are existing attempts. One can regularize the generators by enforcing correspondence between source images and transformed images, such as maintain-

ing mutual information between image patches before and after translation [45] or using a pre-trained model to preserve semantic similarities [59, 9, 54, 24] (which requires extra training inputs that might not be available for most image translation tasks). A common disadvantage of these methods is that, without knowing the ground truth translation functions, one can only guess what content of different semantics should look like in the target domain. Thus, to some extent enforcing an image-to-image (or patch-topatch) correspondence between source and target ones is an ill-posed problem. For instance, by some visually imperceptible clue, objects or patterns from the source domain of one semantic class can be consistently split into those of several semantic classes in the target domain. As a result, the statistical dependencies between input and corresponding output patches remain intact even if semantic flipping happens at various places.

Instead, we propose a constraint on the Lipschitz constant of CycleGAN's generators to improve their semantic robustness. The Lipschitz constants of the generators G and F, denoted L(G) and L(F), are good indicators of their robustness. In specific, they can be expressed as

$$L(G) = \max_{x} \left\| J_x[G(x)] \right\|_{op} \tag{5}$$

$$L(F) = \max_{y} \left\| J_y[F(y)] \right\|_{op} \tag{6}$$

As G and F are enforced to be bijective via the cycle consistency constraints, we also have the equivalent form

$$L(G) = \max_{F(y)} \left\| J_{F(y)}[G(F(y))] \right\|_{op}$$
 (7)

$$L(F) = \max_{G(x)} \left\| J_{G(x)}[F(G(x))] \right\|_{op}$$
 (8)

where  $J[\cdot]$  is the Jacobian matrix and  $||\cdot||_{op}$  is the operator norm. We then penalize the large value of L(G) and L(F). When we choose Euclidean distance as the metric for the image space  $\mathbb{R}^{H\times W\times 3}$ , the corresponding  $||\cdot||_{op}$  is the spectral norm  $||\cdot||_2$ . Since the actual image domains are unknown (we only have access to the sampled training set), we use the gradient penalty technique as in [23] to regularize the empirical estimations of L(G) and L(F) over the training data. However, computing the full Jocabian is very expensive, and so we first aggregate the mean of gradients of a randomly sampled  $S\times S\times S$  region (S is a hyper-parameter) in the transformed image and instead penalize its Euclidean norm. Formally, given an input x and a sampled region  $\mathcal{R}$ , our proposed regularizers are:

$$R(G) = \left\| \nabla_x \mathop{\mathbb{E}}_{(i,j,k) \in \mathcal{R}} G(x)[i,j,k] \right\|_2 \tag{9}$$

$$R(F) = \left\| \nabla_x \mathop{\mathbb{E}}_{(i,j,k) \in \mathcal{R}} F(G(x))[i,j,k] \right\|_2 \tag{10}$$

which are optimized during CycleGAN training w.r.t. weights of G and F, respectively.

# 3.4. Effective Receptive Fields of L-CycleGANs

Before delving into Sec. 4 to demonstrate how our approach reduces semantic flipping, we study the effects of the proposed regularizers on generators. We compare the effective receptive field (ERF) [41] of generators in CycleGAN with or w/o Lipschitz regularization. In specific, we train generator G w/o regularizers and  $G_r$  with regularizers on the Google Map to Aerial Photo dataset [28]. We compute the ERF as a map of on average how sensitive each pixel in the input image is w.r.t. the central pixel of the transformed image. We visualize ERFs by first calculating the gradient of the central pixel of the transformed image (averaged over the RGD channels) w.r.t. the input image and then its Euclidean norm, pixel by pixel, for all the input coordinates. Since CycleGAN has its computed ERF much higher in pixel intensity, for better visualization we clip pixels for a maximum of 1.0. As illustrated in Figure 3, we find that the ERF is reasonably smaller and more concentrated for  $G_r$  compared to G. The normally trained generator has an unnecessarily high dependency on the surrounding area of the input images.

Although for semantic robustness, usually, perturbations occur not by manual injection (as in adversarial robustness) but by the intrinsic diversity of the image distributions, we also try to evaluate our approach in the case of adversarial attacks. We add a small adversarial object to the input image as  $10 \times 10$  patch by cropping the aforementioned gradients generated when computing ERFs and clipping them to have infinity norm as 1. We demonstrate in Figure 3 that  $G_r$  still produces images of good quality whereas G fails to do so.

As adversarial attacks are beyond the scope of this paper, we do not delve deeper.

# 3.5. Comparisons to DistanceGAN/HarmonicGAN

Primarily focused on one-sided image translation, DistanceGAN [8] enforces a distance-preserving mapping between the source and the target domains, based on the intuition that visual distance between source images and that between the corresponding transformed images should be highly correlated. Its regularizer  $R_{dist}(G)$  is

$$R_{dist}(G) = \mathbb{E}_{x_1, x_2} |d_X(x_1, x_2) - d_Y(G(x_1), G(x_2))|$$

where  $x_1, x_2 \sim X$  and  $d_X, d_Y$  are (standardized) L1 distance in the two domains. HarmonicGAN [68] shares this intuition and proposes a slightly more sophisticated patched-based correlation term (omitted here). Our proposed Lipschitz regularizer can be justified similarly. we can derive the counterparts for R(G) / R(F) as

$$R(G) = \mathbb{E}_{x_1, x_2} \frac{d(G(x_1), G(x_2))}{d(x_1, x_2)}$$

Our approach has three clear advantages. Firstly, the enforcement in DistanceGAN and HarmonicGAN can be too restrictive. When the aforementioned intuition is violated as distant source images correspond to not so distant target images, this enforcement that the two distances are highly correlated will result in artifacts. On the contrary, Lipschitz regularizer focuses on large distortions; it allows contraction mappings. This scenario is not uncommon since, within one dataset, some objects/scenes have visually more diverse source images than target ones while some have not. Secondly, both methods' regularizers work on fixed-sized images (entire images for DistanceGAN and fixed-size patches for HarmonicGAN), while R(G) works on the effective receptive field of the generators whose size is adapted to the input images. This makes R(G) much more flexible. Thirdly, our approach enjoys the extra benefits of less vulnerability to noises for the generators.

We have not included DistanceGAN in our experiments as empirically [45] shows that on various datasets it is outperformed by at least one of our baselines.

# 4. Experiments

In this section, we demonstrate how our proposed Lipschitz regularization improves CycleGAN for unpaired image-to-image translation by effectively alleviating the aforementioned semantic flipping problem. Our method performs consistent and robust transformations, outperforming existing GAN-based approaches both qualitatively and quantitatively.

We choose CycleGAN [71], a two-sided method, Gc-GAN [19] and CUT [45], both one-sided methods, as baselines, as they are shown to achieve outstanding performance in standard unpaired image translation tasks compared to other existing work. We evaluate on 5 translation tasks.

### 4.1. Quantitative Evaluation

### **4.1.1** GTA $\rightarrow$ Cityscapes

Cityscapes [14] is a real-world dataset of street-view images, quite popular for semantic segmentation benchmark. It contains 2975 training images, each with original resolution  $2048 \times 1024$ . We resize each of them to  $1024 \times$ 512. GTA5 [52] is a dataset of 24966 synthesized images from the game Grand Theft Auto 5 with original resolution  $1914 \times 1052$ . It contains various scenes in the city with diverse weather and illumination conditions, and similarly, we resize all images to  $1024 \times 512$  for both training and evaluation. The GTA to Cityscapes translation setup is widely used in domain adaptation [62, 25, 24]. Though, most of the existing approaches rely on access to the segmentation labels on the GTA dataset, which we do not assume. Furthermore, work such as CUT [45] utilizes a much larger training set of the Cityscapes dataset (the one with coarse annotations that contains around 20K images).

During the training process, we randomly crop inputs from both domains into  $400 \times 400$  patches. During inference, we apply the learned models on the whole images. We randomly select 500 images from the GTA dataset as the test set and the remaining 24466 for training. We adopt the semantic segmentation metrics used in [45] to measure the quality of the transformed images. We use a light-weight DeepLab [11] model trained on the Cityscapes semantic segmentation task to compute the average pixel prediction accuracy (PixelAcc) and mean intersection-over-union over the 19 classes in Cityscapes (MeanIoU). See Appendix for more details. The numerical results in Table 1 show that our L-CycleGAN has a better performance compared to existing work in both metrics. Visual results in Figure 5 further illustrate its clear advantage of dealing with semantic flipping which other GAN-based methods suffer from.

method	PixelAcc (%)	MeanIoU (%)
CycleGAN	69.02	24.56
GcGAN	63.55	21.93
CUT	67.52	26.92
L-CycleGAN	70.82	28.64

Table 1. Pixel prediction accuracy (PixelAcc) and Mean IoU evaluated on the GTA to Cityscapes task. The best performing entries are highlighted in bold.

#### **4.1.2** Google Map $\rightarrow$ Aerial Photo

The Google Maps dataset [28] contains in total 2194 (map, aerial photo) pairs of images around New York City and is widely used in both paired and unpaired image translation [28, 71, 19]. The dataset is split into 1096 pairs and 1098 pairs for training and test sets, respectively. While our paper focuses on unpaired image translation where the semantic statistics can be quite different across domains, this dataset is originally designed for paired image translation, constructed in a way that gives perfect matching semantic distributions. To deal with this, we sub-sample 500 map images and another 500 aerial photos as our training data, between which there is a reasonable level of statistical difference. In specific, for each of the 1096 pairs, we calculate its score as the average pixel value (for simplicity, over both spatial coordinates and RGB channels) of the map image. This score serves as a rough estimator of how much area is attributed to buildings in the image pair. We then sort all the pairs in the training set by their score from low to high. We construct the set of map images by randomly sampling 350 from one-third of the pairs with highest scores, 100 from the middle third, and another 50 from one third with the lowest scores. On the contrary, for aerial photos, we randomly sample 50, 100, and 350 from the three portions. As a result, on average map images contain more buildings than aerial photos. We use all 1098 test set pairs for evaluation.

The training set has each image resized to  $256 \times 256$ . For quantitative evaluations, we measure the quality of generated aerial photos by average Rooted Mean Square Error (RMSE) and pixel accuracy (%). We follow the protocol in [19] that, given a ground truth pixel  $p_i = (r_i, g_i, b_i)$  and its corresponding predicted value  $p_i' = (r_i', g_i', b_i')$ , the prediction accuracy of  $p_i'$  is defined as  $\mathbb{1}_{\delta}(p_i')$ :

$$\mathbb{1}_{\delta}(p_i') = \begin{cases} 1 & \text{if } \max\left(\left|r_i - r_i'\right|, \left|g_i - g_i'\right|, \left|b_i - b_i'\right|\right) < \delta \\ 0 & \text{otherwise} \end{cases}$$

Since translating map images to aerial photos is more challenging than that in the other direction and our sub-sampling increases the modeling difficulty, we use a larger  $\delta$  here ( $\delta_1=30,\ \delta_2=50$ ) to measure the prediction accuracy compared to the one used in [19]. Table 2 demonstrates our approach can effectively reduce the semantic flipping, preserving more semantic information than the baselines. The visual improvement is illustrated in Figure 5.

Besides the aforementioned two tasks, we further perform qualitative evaluations on the following three datasets. As displayed in Figure 6, for all datasets L-CycleGAN generates better images compared to the baselines.

**Horse**  $\rightarrow$  **Zebra** A famous object transfiguration dataset that contains images randomly sampled from ImageNet [15] using the keywords wild horse and zebra. We use the

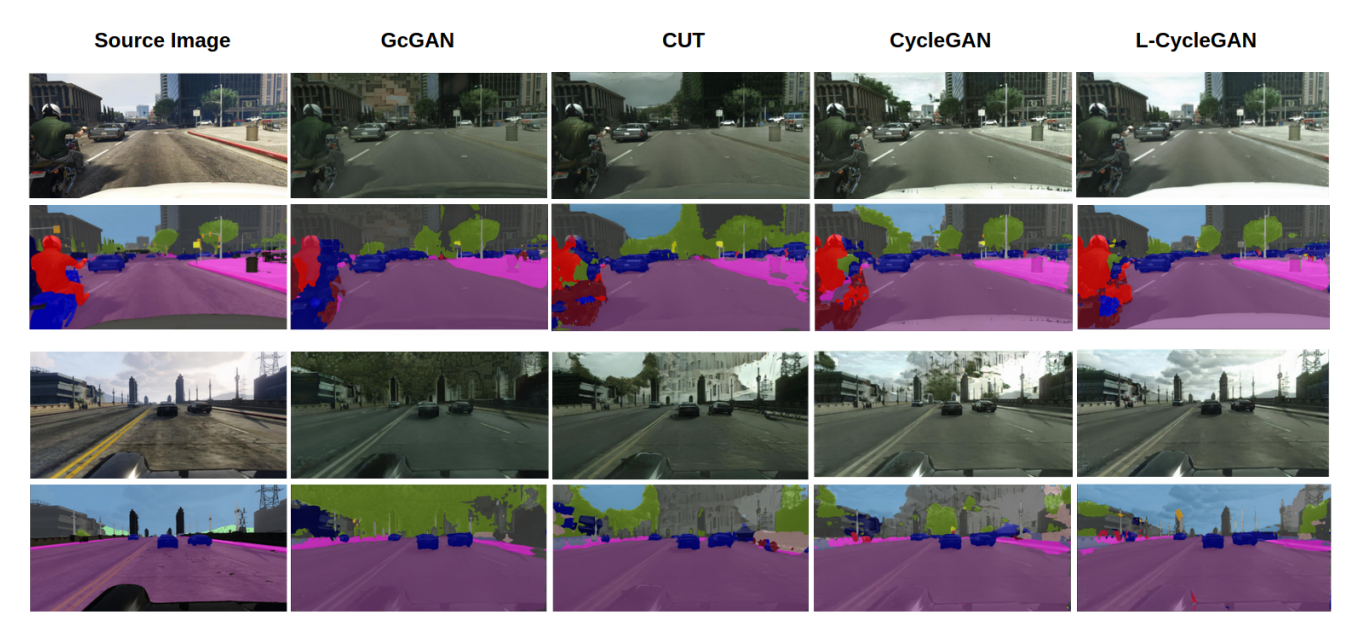


Figure 4. Visual results of the GTA to Cityscapes translation task. The first and third rows are input and transformed images. The second and fourth rows are the corresponding (overlaid) ground truth and predicted segmentation masks. Clearly, our method produces transformed images of better quality that lead to more accurate predictions by the pre-trained DeepLab model.



Figure 5. Visual results of the Google Maps dataset. Ours achieves good quality whereas others suffer from semantic flipping.

method	RMSE	$acc (\delta_1)$	$acc (\delta_2)$
CycleGAN	49.61	44.11	67.68
GcGAN	53.71	44.48	66.62
CUT	53.16	45.94	67.94
L-CycleGAN	49.31	46.55	69.26

Table 2. Average rooted mean square error (RMSE) and pixel prediction accuracy (%) of two different  $\delta$  evaluated on the Google Map to Aerial Photo dataset, with best entries highlighted in bold.

version taken from official TensorFlow Datasets that contains 1067 and 1334 training images for horses and zebras, respectively. All training images are resized to  $256 \times 256$ .

Summer ≒ Winter A collection of photos of Yosemite downloaded from Flickr, originally constructed by authors of CycleGAN. Similarly, we use the TensorFlow version here, which contains 1231 summer images and 962 winter

images for training, each resized to  $256 \times 256$ .

**Day**  $\rightarrow$  **Night** A dataset of outdoor scenes used in [28, 19]. While the original dataset consists of aligned and paired images, we select 1418 day images from 33 cameras and 391 night images from another 33 cameras so that the scenes between two domains have different semantic distribution. Again, all training images are resized to  $256 \times 256$ .

# 4.3. Implementation details

Please refer to the Appendix for full details.

**Network Architectures** For L-CycleGAN, we follow the setup of CycleGAN, which uses the least square loss [42], ResNet-based generators [31] with 9 residual blocks, and patch-based discriminators [28]. We adopt the identity loss (Eqn. 4) as they reduce color distortions [71]. To make it a fair comparison, we also add it for CycleGAN training.

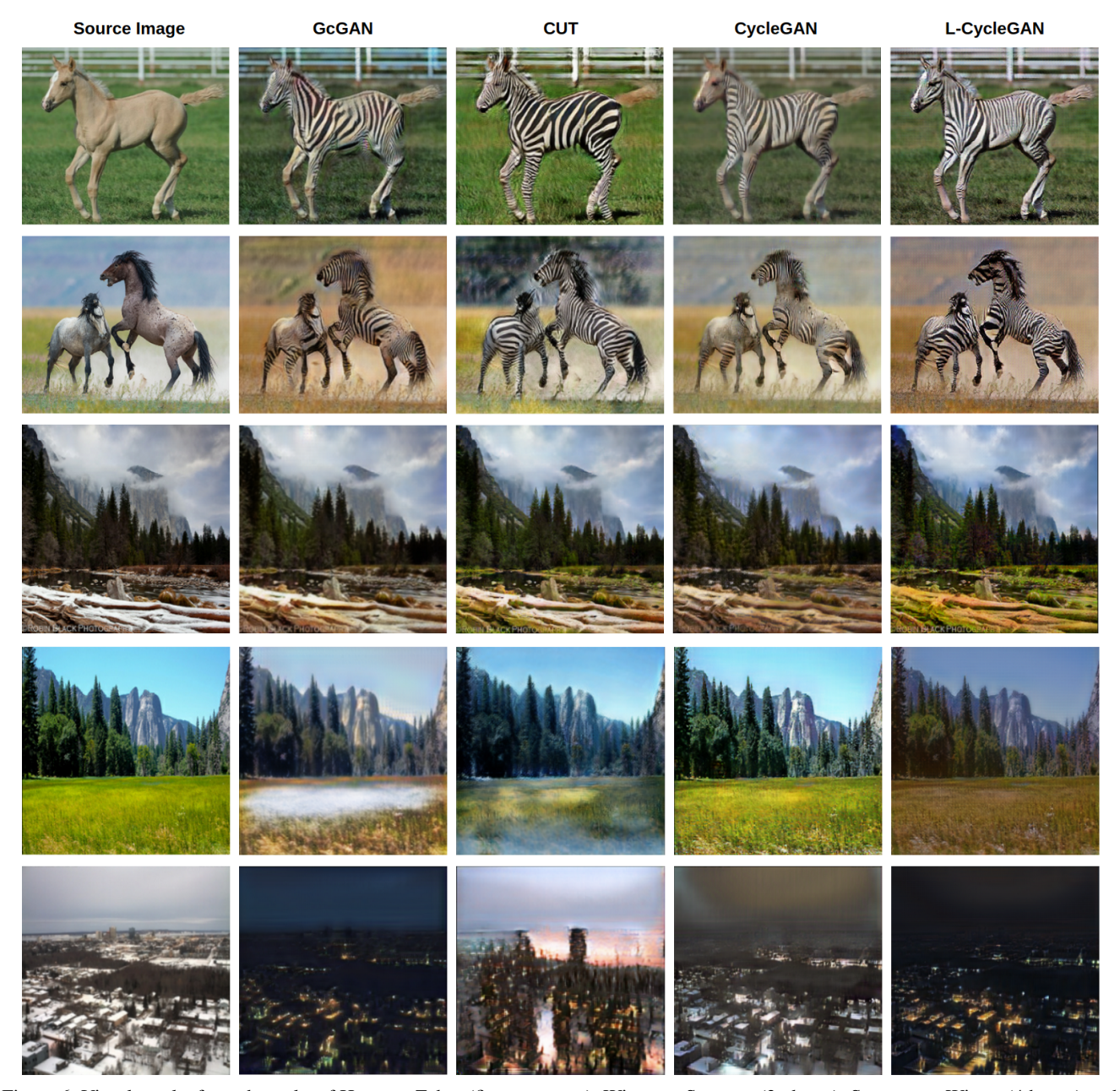


Figure 6. Visual results from the tasks of Horse to Zebra (first two rows), Winter to Summer (3nd row), Summer to Winter (4th row) and Day to Night (5th row). Our proposed L-CycleGAN learns more consistent transformations with less semantic flipping.

**Training Details** Like the strategy in CycleGAN training, we keep an image buffer of size 50 to update the discriminators for better training stability [54]. In all experiments, we follow the default setting of CycleGAN to set the coefficient of cycle loss (Eqn. 3) as 10, that of the identity loss (Eqn. 4) as 5, to use Adam optimizer [35] with the same parameters and initial learning rate (0.0002). For simplicity, we train all models including the baselines for 100K iterations with batch size 2 for all datasets, except that for GTA to

Cityscapes we use batch size 4 and train 125K iterations.

**Hyper-parameters** The major hyper-parameters in L-CycleGAN are S, the size of the sampled regions for aggregating the gradients in computing the Lipschitz regularizers R(G), R(F) (see Sec. 3.3), and the associated coefficients  $\lambda_{R(G)}, \lambda_{R(F)}$ . We search S in  $\{1, 4, 8, 16, 32, 64, 128\}$ ,  $\lambda_{R(G)}, \lambda_{R(F)}$  in  $\{0, 0.01, 0.03, 0.1, 0.3, 1.0, 3.0, 10.0\}$ .

#### 5. Conclusion

In this paper, we tackle the semantic flipping problem in unpaired image translation. We provide two underlying causes for the issue: (1) the source and the target domains have different semantic statistics, and (2) the excessive expressiveness of the generators. Based on our analysis, we propose a simple yet effective solution, namely Lipschitz regularized CycleGAN. In essence, we penalize large Lipschitz constant of the generators, effectively improving the robustness of CycleGAN and thus alleviating semantic flipping. Both quantitative and qualitative evaluations on multiple datasets suggest that our approach produce better and more consistent translations than other GAN-based methods.

#### References

- [1] Naveed Akhtar and Ajmal Mian. Threat of adversarial attacks on deep learning in computer vision: A survey. *IEEE Access*, 6:14410–14430, 2018. 2
- [2] Antreas Antoniou, Amos Storkey, and Harrison Edwards. Data augmentation generative adversarial networks. arXiv preprint arXiv:1711.04340, 2017. 2
- [3] Martin Arjovsky, Soumith Chintala, and Léon Bottou. Wasserstein gan. arXiv preprint arXiv:1701.07875, 2017.
- [4] Sanjeev Arora, Rong Ge, Yingyu Liang, Tengyu Ma, and Yi Zhang. Generalization and equilibrium in generative adversarial nets (gans). *arXiv preprint arXiv:1703.00573*, 2017.
- [5] Sanjeev Arora, Rong Ge, Behnam Neyshabur, and Yi Zhang. Stronger generalization bounds for deep nets via a compression approach. In *International Conference on Machine Learning*, pages 254–263, 2018.
- [6] Peter L Bartlett, Dylan J Foster, and Matus J Telgarsky. Spectrally-normalized margin bounds for neural networks. In Advances in Neural Information Processing Systems, pages 6240–6249, 2017.
- [7] Dina Bashkirova, Ben Usman, and Kate Saenko. Adversarial self-defense for cycle-consistent gans. In Advances in Neural Information Processing Systems, pages 637–647, 2019. 2
- [8] Sagie Benaim and Lior Wolf. One-sided unsupervised domain mapping. In *Advances in neural information processing systems*, pages 752–762, 2017. 2, 5
- [9] Konstantinos Bousmalis, Nathan Silberman, David Dohan, Dumitru Erhan, and Dilip Krishnan. Unsupervised pixellevel domain adaptation with generative adversarial networks. In *Proceedings of the IEEE conference on computer* vision and pattern recognition, pages 3722–3731, 2017. 2, 4
- [10] Konstantinos Bousmalis, George Trigeorgis, Nathan Silberman, Dilip Krishnan, and Dumitru Erhan. Domain separation networks. In *Advances in neural information processing systems*, pages 343–351, 2016. 2
- [11] Liang-Chieh Chen, George Papandreou, Florian Schroff, and Hartwig Adam. Rethinking atrous convolution for semantic image segmentation. arXiv preprint arXiv:1706.05587, 2017. 6

- [12] Xi Chen, Yan Duan, Rein Houthooft, John Schulman, Ilya Sutskever, and Pieter Abbeel. Infogan: Interpretable representation learning by information maximizing generative adversarial nets. In *Advances in neural information processing* systems, pages 2172–2180, 2016. 2
- [13] Casey Chu, Andrey Zhmoginov, and Mark Sandler. Cyclegan, a master of steganography. *arXiv preprint arXiv:1712.02950*, 2017. 1, 2, 3
- [14] Marius Cordts, Mohamed Omran, Sebastian Ramos, Timo Rehfeld, Markus Enzweiler, Rodrigo Benenson, Uwe Franke, Stefan Roth, and Bernt Schiele. The cityscapes dataset for semantic urban scene understanding. In *Proceedings of the IEEE conference on computer vision and pattern recognition*, pages 3213–3223, 2016. 3, 6
- [15] J. Deng, W. Dong, R. Socher, L.-J. Li, K. Li, and L. Fei-Fei. ImageNet: A Large-Scale Hierarchical Image Database. In CVPR09, 2009. 6
- [16] Chris Donahue, Julian McAuley, and Miller Puckette. Adversarial audio synthesis. arXiv preprint arXiv:1802.04208, 2018.
- [17] Vincent Dumoulin, Ishmael Belghazi, Ben Poole, Olivier Mastropietro, Alex Lamb, Martin Arjovsky, and Aaron Courville. Adversarially learned inference. arXiv preprint arXiv:1606.00704, 2016. 2
- [18] Gintare Karolina Dziugaite and Daniel M Roy. Computing nonvacuous generalization bounds for deep (stochastic) neural networks with many more parameters than training data. arXiv preprint arXiv:1703.11008, 2017. 2
- [19] Huan Fu, Mingming Gong, Chaohui Wang, Kayhan Bat-manghelich, Kun Zhang, and Dacheng Tao. Geometry-consistent generative adversarial networks for one-sided unsupervised domain mapping. In *Proceedings of the IEEE Conference on Computer Vision and Pattern Recognition*, pages 2427–2436, 2019. 2, 6, 7
- [20] Ian Goodfellow, Jean Pouget-Abadie, Mehdi Mirza, Bing Xu, David Warde-Farley, Sherjil Ozair, Aaron Courville, and Yoshua Bengio. Generative adversarial nets. In *Advances* in neural information processing systems, pages 2672–2680, 2014. 2
- [21] Ian J Goodfellow, Jonathon Shlens, and Christian Szegedy. Explaining and harnessing adversarial examples. arXiv preprint arXiv:1412.6572, 2014. 2
- [22] Tianyu Gu, Brendan Dolan-Gavitt, and Siddharth Garg. Badnets: Identifying vulnerabilities in the machine learning model supply chain. *arXiv preprint arXiv:1708.06733*, 2017.
- [23] Ishaan Gulrajani, Faruk Ahmed, Martin Arjovsky, Vincent Dumoulin, and Aaron C Courville. Improved training of wasserstein gans. In Advances in neural information processing systems, pages 5767–5777, 2017. 5
- [24] Judy Hoffman, Eric Tzeng, Taesung Park, Jun-Yan Zhu, Phillip Isola, Kate Saenko, Alexei Efros, and Trevor Darrell. Cycada: Cycle-consistent adversarial domain adaptation. In *International conference on machine learning*, pages 1989– 1998. PMLR, 2018. 1, 2, 4, 6
- [25] Judy Hoffman, Dequan Wang, Fisher Yu, and Trevor Darrell. Fcns in the wild: Pixel-level adversarial and constraint-based adaptation. arXiv preprint arXiv:1612.02649, 2016. 6

- [26] Shanjiaoyang Huang, Weiqi Peng, Zhiwei Jia, and Zhuowen Tu. One-pixel signature: Characterizing cnn models for backdoor detection. arXiv preprint arXiv:2008.07711, 2020.
- [27] Xun Huang, Ming-Yu Liu, Serge Belongie, and Jan Kautz. Multimodal unsupervised image-to-image translation. In Proceedings of the European Conference on Computer Vision (ECCV), pages 172–189, 2018. 2
- [28] Phillip Isola, Jun-Yan Zhu, Tinghui Zhou, and Alexei A Efros. Image-to-image translation with conditional adversarial networks. In *Proceedings of the IEEE conference on* computer vision and pattern recognition, pages 1125–1134, 2017. 2, 5, 6, 7
- [29] Zhiwei Jia and Hao Su. Information-theoretic local minima characterization and regularization. arXiv preprint arXiv:1911.08192, 2019.
- [30] Yiding Jiang, Dilip Krishnan, Hossein Mobahi, and Samy Bengio. Predicting the generalization gap in deep networks with margin distributions. In *International Conference on Learning Representations*, 2019. 2
- [31] Justin Johnson, Alexandre Alahi, and Li Fei-Fei. Perceptual losses for real-time style transfer and super-resolution. In European conference on computer vision, pages 694–711. Springer, 2016. 2, 7
- [32] Tero Karras, Timo Aila, Samuli Laine, and Jaakko Lehtinen. Progressive growing of gans for improved quality, stability, and variation. arXiv preprint arXiv:1710.10196, 2017. 2
- [33] Tero Karras, Samuli Laine, and Timo Aila. A style-based generator architecture for generative adversarial networks. In *Proceedings of the IEEE conference on computer vision and pattern recognition*, pages 4401–4410, 2019. 2
- [34] Taeksoo Kim, Moonsu Cha, Hyunsoo Kim, Jung Kwon Lee, and Jiwon Kim. Learning to discover cross-domain relations with generative adversarial networks. arXiv preprint arXiv:1703.05192, 2017. 2
- [35] Diederik P Kingma and Jimmy Ba. Adam: A method for stochastic optimization. arXiv preprint arXiv:1412.6980, 2014. 8
- [36] Christian Ledig, Lucas Theis, Ferenc Huszár, Jose Caballero, Andrew Cunningham, Alejandro Acosta, Andrew Aitken, Alykhan Tejani, Johannes Totz, Zehan Wang, et al. Photorealistic single image super-resolution using a generative adversarial network. In *Proceedings of the IEEE conference on* computer vision and pattern recognition, pages 4681–4690, 2017.
- [37] Minjun Li, Haozhi Huang, Lin Ma, Wei Liu, Tong Zhang, and Yugang Jiang. Unsupervised image-to-image translation with stacked cycle-consistent adversarial networks. In *Proceedings of the European conference on computer vision* (ECCV), pages 184–199, 2018. 2
- [38] Xiaodan Liang, Hao Zhang, and Eric P Xing. Generative semantic manipulation with contrasting gan. *arXiv preprint arXiv:1708.00315*, 2017. 1, 2
- [39] Ming-Yu Liu, Thomas Breuel, and Jan Kautz. Unsupervised image-to-image translation networks. In *Advances in neural* information processing systems, pages 700–708, 2017.

- [40] Ming-Yu Liu and Oncel Tuzel. Coupled generative adversarial networks. In *Advances in neural information processing systems*, pages 469–477, 2016. 2
- [41] Wenjie Luo, Yujia Li, Raquel Urtasun, and Richard Zemel. Understanding the effective receptive field in deep convolutional neural networks. Advances in neural information processing systems, 29:4898–4906, 2016. 5
- [42] Xudong Mao, Qing Li, Haoran Xie, Raymond YK Lau, Zhen Wang, and Stephen Paul Smolley. Least squares generative adversarial networks. In *Proceedings of the IEEE international conference on computer vision*, pages 2794–2802, 2017. 2, 3, 7
- [43] Behnam Neyshabur, Ryota Tomioka, and Nathan Srebro. Norm-based capacity control in neural networks. In Conference on Learning Theory, pages 1376–1401, 2015.
- [44] Sebastian Nowozin, Botond Cseke, and Ryota Tomioka. f-gan: Training generative neural samplers using variational divergence minimization. In *Advances in neural information processing systems*, pages 271–279, 2016. 2
- [45] Taesung Park, Alexei A Efros, Richard Zhang, and Jun-Yan Zhu. Contrastive learning for unpaired image-to-image translation. In *European Conference on Computer Vision*, pages 319–345. Springer, 2020. 1, 2, 4, 5, 6
- [46] Deepak Pathak, Philipp Krahenbuhl, Jeff Donahue, Trevor Darrell, and Alexei A Efros. Context encoders: Feature learning by inpainting. In *Proceedings of the IEEE conference on computer vision and pattern recognition*, pages 2536–2544, 2016. 2
- [47] Aaditya Prakash, Nick Moran, Solomon Garber, Antonella DiLillo, and James Storer. Deflecting adversarial attacks with pixel deflection. In Proceedings of the IEEE conference on computer vision and pattern recognition, pages 8571– 8580, 2018. 2
- [48] Guo-Jun Qi. Loss-sensitive generative adversarial networks on lipschitz densities. *International Journal of Computer Vi*sion, 128(5):1118–1140, 2020. 2
- [49] Alec Radford, Luke Metz, and Soumith Chintala. Unsupervised representation learning with deep convolutional generative adversarial networks. *arXiv preprint arXiv:1511.06434*, 2015. 2
- [50] Scott Reed, Zeynep Akata, Xinchen Yan, Lajanugen Logeswaran, Bernt Schiele, and Honglak Lee. Generative adversarial text to image synthesis. arXiv preprint arXiv:1605.05396, 2016.
- [51] Scott E Reed, Yi Zhang, Yuting Zhang, and Honglak Lee. Deep visual analogy-making. In Advances in neural information processing systems, pages 1252–1260, 2015. 2
- [52] Stephan R Richter, Vibhav Vineet, Stefan Roth, and Vladlen Koltun. Playing for data: Ground truth from computer games. In *European conference on computer vision*, pages 102–118. Springer, 2016. 3, 6
- [53] Pouya Samangouei, Maya Kabkab, and Rama Chellappa. Defense-gan: Protecting classifiers against adversarial attacks using generative models. arXiv preprint arXiv:1805.06605, 2018. 2
- [54] Ashish Shrivastava, Tomas Pfister, Oncel Tuzel, Joshua Susskind, Wenda Wang, and Russell Webb. Learning

- from simulated and unsupervised images through adversarial training. In *Proceedings of the IEEE conference on computer vision and pattern recognition*, pages 2107–2116, 2017. 2, 4, 8
- [55] Jure Sokolić, Raja Giryes, Guillermo Sapiro, and Miguel RD Rodrigues. Robust large margin deep neural networks. *IEEE Transactions on Signal Processing*, 65(16):4265–4280, 2017.
- [56] Jiawei Su, Danilo Vasconcellos Vargas, and Kouichi Sakurai. One pixel attack for fooling deep neural networks. *IEEE Transactions on Evolutionary Computation*, 23(5):828–841, 2019.
- [57] Bo Sun, Nian-hsuan Tsai, Fangchen Liu, Ronald Yu, and Hao Su. Adversarial defense by stratified convolutional sparse coding. In *Proceedings of the IEEE Conference on Computer Vision and Pattern Recognition*, pages 11447–11456, 2019.
- [58] Christian Szegedy, Wojciech Zaremba, Ilya Sutskever, Joan Bruna, Dumitru Erhan, Ian Goodfellow, and Rob Fergus. Intriguing properties of neural networks. arXiv preprint arXiv:1312.6199, 2013. 2
- [59] Yaniv Taigman, Adam Polyak, and Lior Wolf. Unsupervised cross-domain image generation. *arXiv preprint arXiv:1611.02200*, 2016. 1, 2, 4
- [60] Hoang Thanh-Tung, Truyen Tran, and Svetha Venkatesh. Improving generalization and stability of generative adversarial networks. arXiv preprint arXiv:1902.03984, 2019.
- [61] Kiran K Thekumparampil, Ashish Khetan, Zinan Lin, and Sewoong Oh. Robustness of conditional gans to noisy labels. In Advances in neural information processing systems, pages 10271–10282, 2018. 2
- [62] Yi-Hsuan Tsai, Wei-Chih Hung, Samuel Schulter, Kihyuk Sohn, Ming-Hsuan Yang, and Manmohan Chandraker. Learning to adapt structured output space for semantic segmentation. In *Proceedings of the IEEE Conference on Com*puter Vision and Pattern Recognition, pages 7472–7481, 2018. 6
- [63] Ting-Chun Wang, Ming-Yu Liu, Jun-Yan Zhu, Andrew Tao, Jan Kautz, and Bryan Catanzaro. High-resolution image synthesis and semantic manipulation with conditional gans. In Proceedings of the IEEE conference on computer vision and pattern recognition, pages 8798–8807, 2018. 2
- [64] Huan Xu and Shie Mannor. Robustness and generalization. Machine learning, 86(3):391–423, 2012.
- [65] Han Zhang, Ian Goodfellow, Dimitris Metaxas, and Augustus Odena. Self-attention generative adversarial networks. In *International Conference on Machine Learning*, pages 7354–7363. PMLR, 2019.
- [66] Han Zhang, Tao Xu, Hongsheng Li, Shaoting Zhang, Xiao-gang Wang, Xiaolei Huang, and Dimitris N Metaxas. Stackgan: Text to photo-realistic image synthesis with stacked generative adversarial networks. In *Proceedings of the IEEE international conference on computer vision*, pages 5907–5915, 2017.
- [67] Pengchuan Zhang, Qiang Liu, Dengyong Zhou, Tao Xu, and Xiaodong He. On the discrimination-generalization tradeoff in gans. arXiv preprint arXiv:1711.02771, 2017.

- [68] Rui Zhang, Tomas Pfister, and Jia Li. Harmonic unpaired image-to-image translation. *arXiv preprint arXiv:1902.09727*, 2019. 2, 5
- [69] Wenda Zhou, Victor Veitch, Morgane Austern, Ryan P. Adams, and Peter Orbanz. Non-vacuous generalization bounds at the imagenet scale: a PAC-bayesian compression approach. In *International Conference on Learning Representations*, 2019. 2
- [70] Zhiming Zhou, Jiadong Liang, Yuxuan Song, Lantao Yu, Hongwei Wang, Weinan Zhang, Yong Yu, and Zhihua Zhang. Lipschitz generative adversarial nets. arXiv preprint arXiv:1902.05687, 2019.
- [71] Jun-Yan Zhu, Taesung Park, Phillip Isola, and Alexei A Efros. Unpaired image-to-image translation using cycleconsistent adversarial networks. In *Proceedings of the IEEE* international conference on computer vision, pages 2223– 2232, 2017. 1, 2, 3, 6, 7